

## Observation of mesoscopic conductance fluctuations in $\text{YBa}_2\text{Cu}_3\text{O}_{7-\delta}$ grain boundary Josephson junctions

A. Tagliacozzo,<sup>1,2</sup> D. Born,<sup>1,2</sup> D. Stornaiuolo,<sup>1,2</sup> E. Gambale,<sup>3</sup> D. Dalena,<sup>3</sup> F. Lombardi,<sup>4</sup> A. Barone,<sup>1,2</sup>  
B. L. Altshuler,<sup>5,6</sup> and F. Tafuri<sup>1,2,3</sup>

<sup>1</sup>*CNR-INFM Coherentia, Università di Napoli Federico II, Napoli, Italy*

<sup>2</sup>*Dipartimento di Scienze Fisiche, Università di Napoli Federico II, Via Cintia, 80125 Napoli, Italy*

<sup>3</sup>*Dipartimento Ingegneria dell'Informazione, Seconda Università di Napoli, Aversa (CE), Italy*

<sup>4</sup>*Department of Microelectronics and Nanoscience, MINA, Chalmers University of Technology, S-41296 Goteborg, Sweden*

<sup>5</sup>*Physics Department, Columbia University, New York, New York 10027, USA*

<sup>6</sup>*NEC Laboratories America Inc., 4 Independence Day, Princeton, New Jersey 08554, USA*

(Received 7 December 2006; published 24 January 2007)

Magnetofluctuations of the normal-state resistance  $R_N$  have been reproducibly observed in high-critical-temperature superconductor (HTS) grain boundary junctions at low temperatures. We attribute them to mesoscopic transport in narrow channels across the grain boundary line. The Thouless energy appears to be the relevant energy scale. Our findings have significant implications for quasiparticle relaxation and coherent transport in HTS grain boundaries.

DOI: [10.1103/PhysRevB.75.012507](https://doi.org/10.1103/PhysRevB.75.012507)

PACS number(s): 74.50.+r, 74.72.Bk, 74.78.Na

Junctions are extremely useful to test very important properties of high-critical-temperature superconductors (HTS's),<sup>1-3</sup> whose nature has not yet been completely established.<sup>4</sup> Recently, high-quality  $\text{YBa}_2\text{Cu}_3\text{O}_{7-\delta}$  (YBCO) grain boundary (GB) Josephson junctions (JJ's) have given the first evidence of a potential to study exciting crucial issues such as macroscopic quantum behaviors, coherence, and dissipation.<sup>5,6</sup> The macroscopic quantum tunneling in such  $d$ -wave devices out of the zero-voltage state has been demonstrated along with the quantization of its energy states.<sup>5</sup> The crossover temperature between quantum and classical regimes was found to be of the order of 40 mK. This is evidence of the fact that despite the short coherence lengths in a highly disordered environment and the presence of low-energy *nodal* quasiparticles (QP's) due to the nodes of the  $d$ -wave order parameter symmetry,<sup>1,3,5</sup> dissipation in a HTS junction does not seem to be as disruptive for the quantum coherence at low temperatures, as one would naively expect. Increasing the available information about the nature of QP's and their relaxation processes is of crucial importance to unveil the mechanism which leads to superconductivity in HTS's.

In this paper we report on transport measurements of YBCO biepitaxial (BP) GB junctions [see the scheme in Fig. 1(a)], which give evidence of conductance fluctuations (CFs) in the magnetoconductance response. To our knowledge, this is the first time that CF's are measured in HTS junctions. Our results prove the appearance of mesoscopic effects in the unusual energy regime  $k_B T \ll \epsilon_c < eV < \Delta$ .<sup>7</sup> Here  $k_B T$  is the thermal energy at temperature  $T$ ,  $\epsilon_c$  is the Thouless energy, which will be introduced below,  $V$  is the applied voltage, and  $\Delta$  is the superconducting gap [ $\approx 20$  meV for YBCO (Ref. 1)].

The progress registered in mesoscopic physics in the last two decades is impressive.<sup>8-10</sup> At low temperatures, quantum coherence can be monitored in the conductance  $G$  of a normal metallic sample of length  $L_x$  attached to two reservoirs. The electron wave packets that carry current in a diffusive wire have a minimum size of the order of  $L_T > L_x \gg l$ . Here  $l$

is the electron mean free path in the wire and  $L_T$  is the thermal diffusion length  $\sqrt{\hbar D/k_B T}$  ( $D$  is the diffusion constant). The first inequality is satisfied at relatively low temperatures as far as  $k_B T \ll \epsilon_c \equiv \hbar D/L_x^2$ . At low voltages ( $eV \ll \epsilon_c$ ), the system is in the regime of universal conductance fluctuations: the variance  $\langle \delta g^2 \rangle$  of the dimensionless conductance  $g = G/(2e^2/\hbar)$  is of the order of unity. Mesoscopic phenomena have been widely investigated even in metallic wires interrupted by tunnel junctions<sup>11</sup> and in Josephson junctions.<sup>12-14</sup> In experiments on Nb/Cu/Nb long junctions,<sup>14</sup> phase coherence mediated by Andreev reflection at the  $S/N$  interfaces has been shown to persist in the whole diffusive metallic channel, several hundreds of nanometers long. Such an effect is robust with respect to energy broadening due to temperature, but it is expected to be fragile to energy relaxation processes induced by the applied voltage. By contrast, in our case, the QP phase coherence time  $\tau_\varphi$  seems not to be limited by energy relaxation due to voltage-induced nonequilibrium. Mesoscopic resistance oscillations are found even for  $eV > \epsilon_c$ , indicating that QP's do not lose coherence at low temperatures, while diffusing across the  $N$  bridge. By plotting the autocorrelation function of the measured CF's in magnetic field  $H$  (see below), we determine  $\epsilon_c$ , in analogy to similar studies of normal metal and semiconductor systems.<sup>10,15</sup> HTS GB JJ's make accessible this regime, which is not commonly achieved by conventional metals and junctions, providing a *direct* measurement of the Thouless energy.

The BP JJ's are obtained at the interface between a (103) YBCO film grown on a (110)  $\text{SrTiO}_3$  substrate and a  $c$ -axis film deposited on a (110)  $\text{CeO}_2$  seed layer [Fig. 1(a)]. The presence of the  $\text{CeO}_2$  produces an additional  $45^\circ$  in-plane rotation of the YBCO axes with respect to the in-plane directions of the substrate. By suitable patterning of the  $\text{CeO}_2$  seed layer, the interface orientation can be varied and tuned to some appropriate transport regime [in Fig. 1(a) we have indicated the two limiting cases of  $0^\circ$  and  $90^\circ$  and an intermediate situation defined by the angle  $\theta$ , in our case  $\theta = 60^\circ$ ].<sup>6,16</sup> We have selected junctions with submicrometer

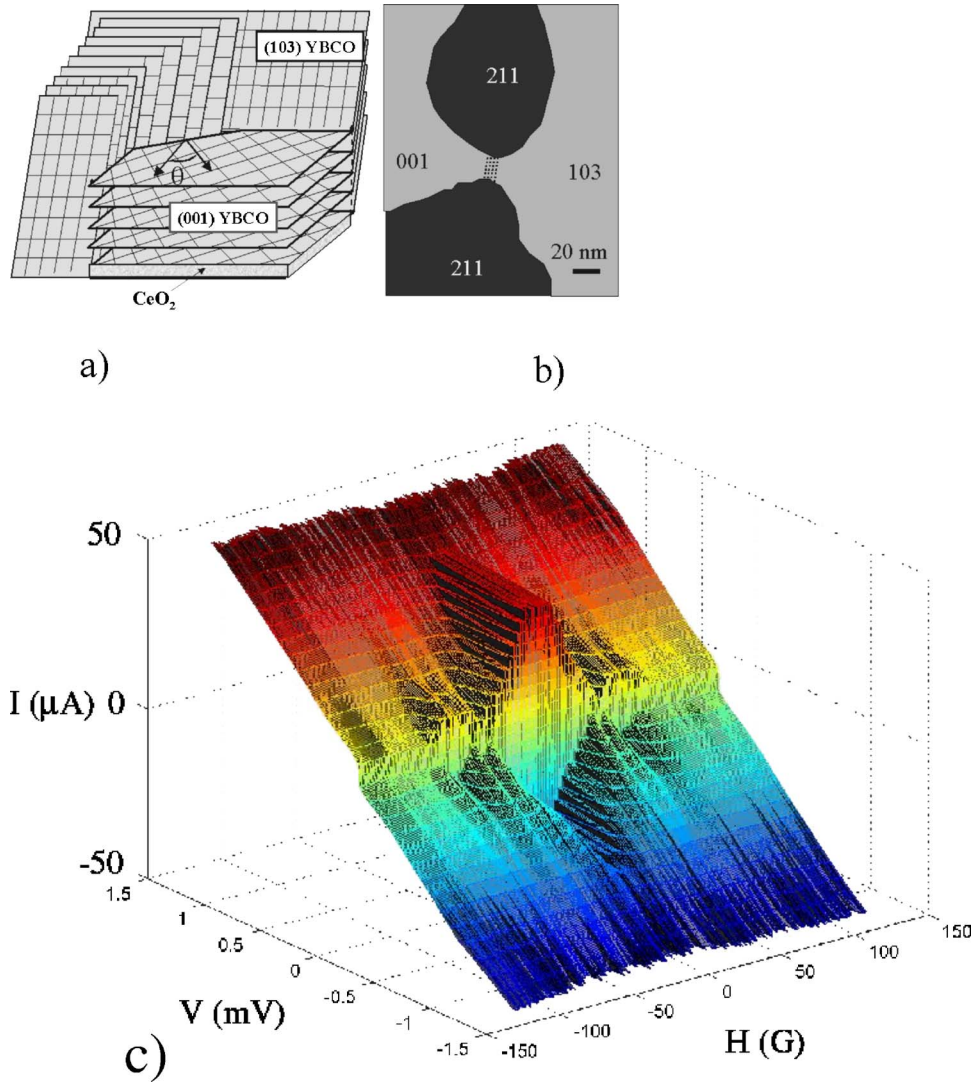


FIG. 1. (Color online) (a) Sketch of the grain boundary structure for three different interface orientations. (b) Sketch of a typical mesoscopic channel, which might be generated at the grain boundary line (dotted lines) because of the presence of impurities. Black regions marked 211 are insulating. In biepitaxial junctions, the impurities may be due to yttrium excess. (c)  $I$ - $V$  curves as a function of the magnetic field  $H$ : the Fraunhofer pattern indicates a uniform interface with critical current density  $J_C \sim 8 \times 10^4$  A/cm<sup>2</sup> at  $T=4.2$  K.

channels, as eventually confirmed by scanning electron microscope analyses, and measured their current-voltage ( $I$ - $V$ ) characteristics, as a function of  $H$  and  $T$ . Standard four-terminal measurements of the  $I$ - $V$  curves and of the differential resistance were made down to 300 mK in a <sup>3</sup>He evaporation cryostat. The electrical lines to the sample are equipped with copper powder microwave low-pass filters (cutoff frequency about 10 GHz) and discrete low-pass  $RC$  filters ( $<1.6$  MHz). The magnetic screening is guaranteed by two Cryoperm screens and a two-layer (Pb/Nb) superconducting screen inside the liquid He Dewar.

We have investigated various samples, but here we focus mostly on the junction characterized by the Fraunhofer magnetic pattern shown in Fig. 1(c), where it is more likely that only one uniform superconducting path is active.<sup>17</sup> In Fig. 1(c) the  $I$ - $V$  curves are reported in a three-dimensional (3D) plot as a function of magnetic field  $H$ . The critical current ( $I_C$ ) oscillations point to a flux periodicity which is roughly consistent with the typical size (10–100 nm) that we expect for our microbridge from structural investigations [see Fig. 1(b)]. We have to take into account that the London penetration depth in the (103)-oriented electrode is of the order of a

few micrometers (much larger than the one in  $c$ -axis YBCO films) (see Ref. 5, for instance).

In low- $T_c$  JJ's,  $R_N$  represents the resistance at a voltage a few times larger than the gap value. This matter is more delicate when dealing with HTS JJ's, because of the deviations from the ideal resistively-shunted-junction-like (RSJ-like) behavior.<sup>2,3</sup> In our case a linear branch typical of the RSJ behavior starts at  $V=5$  mV. Values of  $V$  between 10 mV and 15 mV are representative for the problem we are investigating. We choose  $V \approx 12$  mV for deriving the  $R_N$  vs  $H$  curve, which is reported in Fig. 2 at the temperature  $T=300$  mK in the interval  $[-200$  G, 200 G]. The average resistance  $\bar{R}_N$  over the whole magnetic field range is  $\sim 182$   $\Omega$ . Conductance fluctuations, such as those shown in Fig. 2, become appreciable at temperatures below 900 mK ( $k_B T \ll \hbar I_C / 2e$ ), in the whole magnetic field range. Below 1.2 K, the fluctuations are nonperiodic, and for sure not related to the  $I_C(H)$  periodicity, and have all the typical characteristics of mesoscopic fluctuations. When sweeping  $H$  back, the pattern shows occasionally some hysteresis mostly at high magnetic fields, which we attribute to some delay in the magnetic response. Above 1.2 K, thermal fluctuations

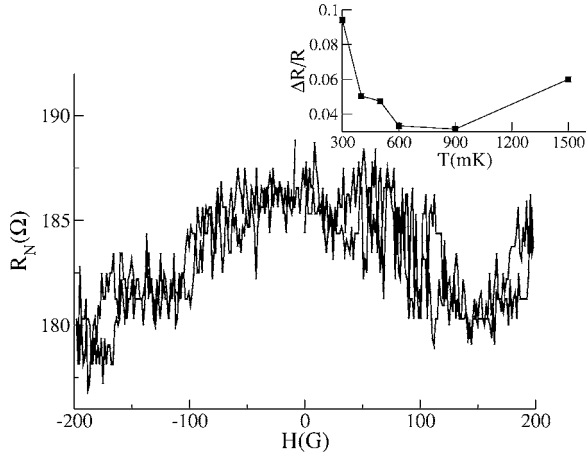


FIG. 2. Resistance  $R_N$  vs  $H$  at  $T=300$  mK. Marked nonperiodic fluctuations are evident. In the inset, the zero-field amplitude of the fluctuations is reported vs  $T$ .

dominate, possibly due to vortices pinned in the superconductor, far from the interface (see the inset in Fig. 2).

We perform the ensemble average of the autocorrelation of the conductance fluctuations  $\delta G \equiv G - \bar{G}_N$  [with  $\bar{G}_N \equiv (\bar{R}_N)^{-1}$ ] over  $H$  (this average will be denoted by  $\langle \dots \rangle_H$ ). We also divide the voltage range  $V \in (10-15$  mV) into  $N_V$  small intervals and take the average in each of them as representative of the autocorrelation on a coarse-grained voltage scale. The resulting average is denoted by  $\langle \dots \rangle$  with no subscript. The autocorrelation of the conductance fluctuations is therefore defined as

$$\begin{aligned} & \langle [G(\Delta V) - \bar{G}_N][G(0) - \bar{G}_N] \rangle \\ & \equiv \frac{1}{N_V} \sum_V \langle [G(V + \Delta V, H) - \bar{G}_N][G(V, H) - \bar{G}_N] \rangle_H. \end{aligned} \quad (1)$$

Its amplitude at  $\Delta V=0$  is  $\sqrt{\langle (\delta G)^2 \rangle} \sim 0.07 \bar{G}_N$  at 300 mK, more than one order of magnitude larger than the noise. The autocorrelation, Eq. (1), is reported in Fig. 3 vs  $\Delta V$  at various temperatures. The plots average over various series of measurements to suppress accidental resistive effects in the superconductor. In spite of the fact that the autocorrelation function, Eq. (1), is measured away from equilibrium in a superconductive system, we find that the data can be fitted resorting to the standard theory for transport of diffusion modes in mesoscopic channels,<sup>18</sup> as the inset of Fig. 3 shows. The effect of the applied  $H$  on the interference is expected to rule out contributions to the conductance fluctuations due to Cooperons. In a normal mesoscopic 3D sample of cross-section area  $L_y L_z$ , the autocorrelation at  $V \rightarrow 0$ , as a function of phase changes  $\Delta \varphi$  induced by external conditions, can be approximated as

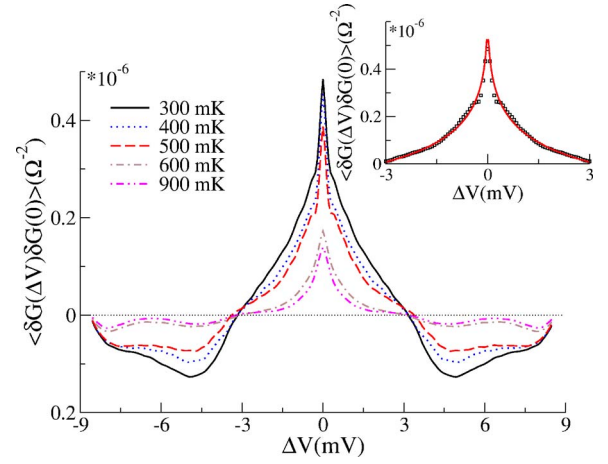


FIG. 3. (Color online) The autocorrelation function, Eq. (1), is derived from experimental data for different temperatures. In the inset the autocorrelation function at  $T=300$  mK is fitted on the basis of Eq. (2) (solid line).

$$\begin{aligned} \langle \delta G(\Delta \varphi) \delta G(0) \rangle &= \sum_{\substack{m=-\infty \\ m \neq 0}}^{\infty} \langle G_m G_{-m} \rangle e^{im\Delta \varphi} \\ &\approx \frac{2N}{3\pi} \left( \frac{2e^2}{h} \right)^2 \frac{\epsilon_c}{k_B T} \frac{L_y L_z}{L_x L_T} \text{Re}\{\ln(1 - e^{-(\xi+i\Delta \varphi)})\} \end{aligned} \quad (2)$$

Here the parameter  $\xi = \pi L_x / L_T$  contains the important information on the channel effective length with respect to  $L_T$  ( $N$  is a constant of the order 1, up to higher orders in  $e^{-|m|\xi}$ , also depending on the system symmetries). In deriving Eq. (2) we have assumed  $k_B T \gg \hbar / \tau_\varphi$  and larger than the level spacing in the submicrobridge.<sup>19</sup> The Fourier components of the autocorrelation  $\langle G_m G_{-m} \rangle$ , in the limit of small  $m$ 's, are  $\langle G_m G_{m'} \rangle \propto \delta_{m', -m} \text{erfc}(\sqrt{|m|} \xi) e^{-|m|\xi} / |m|$ . The exponential integral function  $\text{erfc}$ , together with the  $\delta_{m', -m}$ , arises from the sum over the diffuson modes. In the inset of Fig. 3 the solid line shows the best fit obtained by using Eq. (2) with  $\Delta \varphi = \sqrt{e} \Delta V / \epsilon_c$  and  $\xi = 0.1$ . This value of  $\xi$  is consistent with a  $L_x$  value of the order of 50 nm. The value of  $\epsilon_c$  can be read out of the plot from the half width at its half maximum, giving  $\epsilon_c$  of the order of 1 meV. Equation (2) also displays a node as the data of Fig. 3. However, correlations at larger  $\Delta \varphi$  have to blur out due to other mechanisms of dephasing not included here and cannot follow Eq. (2).

Our plots can be compared to the ones of Ref. 11 obtained for an Al/Al<sub>2</sub>O<sub>3</sub>/Al tunnel junction at  $T=20$  mK,  $V=0.8$  mV in a magnetic field  $H=0.5$  T which drives the junction into the normal state. In Ref. 11, the energy broadening extracted from the experiment,  $\sim \max\{\hbar / \tau_\varphi, \epsilon_c\}$ , is 2.3  $\mu\text{eV}$ , at 20 mK.

It is remarkable that the coherence time which is expected when dephasing is dominated by small-energy-transfer (Nyquist) scattering of nodal QP's [ $\sim \hbar / V$  Ref. 20] is much shorter than  $\hbar / \epsilon_c$ . In our case,  $\langle (\Delta \varphi)^2 \rangle \approx e \Delta V / \epsilon_c \sim 1$  fixes the scale of amplitude of the fluctuations of  $\Delta V$  for carriers diffusing across the bridge. We have found that both tempera-

ture and bias voltages up to 30 meV reduce the amplitude of the CF's and of  $\epsilon_c$ , but they do not wash out the correlations.  $\sqrt{\langle(\delta G/\bar{G}_N)^2\rangle}$  drops with temperature, according to Eq. (2), as probed from the experiment (see inset of Fig. 2).

Given that the thermal diffusion length  $L_T \sim 0.13 \mu\text{m}$  at 1 K [with  $D \sim 20\text{--}24 \text{ cm}^2/\text{s}$  for YBCO (Ref. 21)], the condition  $L_x < L_T$  is certainly met, thus confirming that  $\epsilon_c$  is the relevant energy scale. The phase coherence length exceeds the size of the microbridge, and therefore thermal decoherence can be ruled out. Hence, not only the interference of tunneling currents takes place, which provides the Fraunhofer pattern of Fig. 1(c), but also the quantum interference of QP's returning back to the junction in their diffusive motion at the GB. We believe that this is the first time that quantum interference of quasiparticles in HTS junctions appears and that mesoscopic scales can be identified.

As a final remark, our measurements show that  $\epsilon_c$  is the relevant energy scale for the supercurrent as well. Indeed, we find that  $eI_c R_N$  and  $\epsilon_c$  are of the same order of magnitude, in agreement with the typical values measured in HTS JJ's (Refs. 2 and 3) and the results on diffusive phase-coherent normal-metal SNS weak links.<sup>14,22</sup> This feature gives additional consistency to the whole picture, relating the critical current, which is mediated by subgap Andreev reflection, to the transport properties at high voltages. The coherent diffusive regime across the S/N/S channel of our GB junctions persists even at larger voltage bias  $\Delta > eV > \epsilon_c$  and is the

dominating conduction mechanism. Hence, microscopic features of the weak link appear as less relevant, in favor of mesoscopic, nonlocal properties. The fact that the dominant energy scale is found to be  $\epsilon_c \sim 1 \text{ meV}$  sets a lower bound to the relaxation time at low  $T$  for QP's of energy even 40 times larger, of the order of picoseconds. It has been argued that antinodal QP's may require slow diffusive drift of momentum along the Fermi surface towards the nodes of the  $d$ -wave gap.<sup>21,23</sup>

In conclusion, important attributes of the role of grain boundaries emerge in the transport in HTS junctions and in particular of narrow self-protected channels formed in the complex growth of the oxide grain boundary.<sup>2,3,24,25</sup> We have given evidence of conductance fluctuations in HTS grain boundary Josephson junctions constricted by one single microbridge at low temperatures. CF's are the signature of a coherent diffusive regime. Our results seem to suggest an unexpectedly long QP phase coherence time and represents another strong indication that the role of dissipation in HTS's has to be revised.

Work partially supported by the ESF projects "II-Shift" and "QUACS" and by MIUR funds (Italy). Numerical help by B. Jouault and P. Lucignano, as well as discussions with T. Bauch, C. Biagini, G. Campagnano, J. R. Kirtley, A. Mirlin, H. Poithier, and Y. Nazarov are gratefully acknowledged.

- 
- <sup>1</sup>C. C. Tsuei and J. R. Kirtley, *Rev. Mod. Phys.* **72**, 969 (2000).  
<sup>2</sup>H. Hilgenkamp and J. Mannhart, *Rev. Mod. Phys.* **74**, 485 (2002).  
<sup>3</sup>F. Tafuri and J. R. Kirtley, *Rep. Prog. Phys.* **68**, 2573 (2005).  
<sup>4</sup>D. A. Bonn, *Nat. Phys.* **2**, 159 (2006); A. J. Leggett, *ibid.* **2**, 134 (2006); P. W. Anderson, *Science* **288**, 480 (2000).  
<sup>5</sup>T. Bauch, T. Lindstrom, F. Tafuri, G. Rotoli, P. Delsing, T. Claesson, and F. Lombardi, *Science* **311**, 57 (2006); T. Bauch *et al.*, *Phys. Rev. Lett.* **94**, 087003 (2005).  
<sup>6</sup>F. Lombardi, F. Tafuri, F. Ricci, F. Miletto Granozio, A. Barone, G. Testa, E. Sarnelli, J. R. Kirtley, and C. C. Tsuei, *Phys. Rev. Lett.* **89**, 207001 (2002).  
<sup>7</sup>T. Ludwig, Ya. M. Blanter, and A. D. Mirlin, *Phys. Rev. B* **70**, 235315 (2004).  
<sup>8</sup>B. L. Altshuler, *Pis'ma Zh. Eksp. Teor. Fiz.* **41**, 530 (1985) [*JETP Lett.* **41**, 648 (1985)]; P. A. Lee and A. D. Stone, *Phys. Rev. Lett.* **55**, 1622 (1985).  
<sup>9</sup>B. L. Altshuler and P. A. Lee, *Phys. Today* **41**, 36 (1988); R. A. Webb and S. Washburn, *ibid.* **41**, 46 (1988); For a review see *Mesoscopic Phenomena in Solids*, edited by B. L. Altshuler, P. A. Lee, and R. A. Webb (North-Holland, New York, 1991).  
<sup>10</sup>Y. Imry, *Introduction to Mesoscopic Physics* (Oxford University Press, Oxford, 1997).  
<sup>11</sup>A. van Oudenaarden, M. H. Devoret, E. H. Visscher, Yu. V. Nazarov, and J. E. Mooij, *Phys. Rev. Lett.* **78**, 3539 (1997).  
<sup>12</sup>H. Takayanagi, J. Bindslev Hansen, and J. Nitta, *Phys. Rev. Lett.* **74**, 166 (1995).  
<sup>13</sup>J. P. Heida, B. J. van Wees, T. M. Klapwijk, and G. Borghs, *Phys. Rev. B* **60**, R13135 (1999).  
<sup>14</sup>P. Dubos, H. Courtois, B. Pannetier, F. K. Wilhelm, A. D. Zaikin, and G. Schön, *Phys. Rev. B* **63**, 064502 (2001).  
<sup>15</sup>F. Hohls, U. Zeitler, and R. J. Haug, *Phys. Rev. B* **66**, 073304 (2002).  
<sup>16</sup>F. Tafuri, F. Miletto Granozio, F. Carillo, A. Di Chiara, K. Verbist, and G. Van Tendeloo, *Phys. Rev. B* **59**, 11523 (1999).  
<sup>17</sup>For a nonuniform current distribution along the GB that may occur if different paths were present, relevant deviations from the Fraunhofer pattern of Fig. 1(c) would appear [see, e.g., A. Barone and G. Paternò, *Physics and Applications of the Josephson Effect* (Wiley, New York, 1982)].  
<sup>18</sup>P. A. Lee, A. D. Stone, and H. Fukuyama, *Phys. Rev. B* **35**, 1039 (1987).  
<sup>19</sup>B. L. Altshuler and B. Z. Spivak, *Zh. Eksp. Teor. Fiz.* **92**, 609 (1987) [*Sov. Phys. JETP* **65**, 343 (1987)].  
<sup>20</sup>G. L. Ingold and Yu. V. Nazarov, in *Single Charge Tunneling*, edited by H. Grabert and M. H. Devoret, Vol. 294 of NATO Advanced Study Institute, Series B: Physics (Plenum Press, New York, 1992).  
<sup>21</sup>N. Gedik, J. Orenstein, Ruixing Liang, D. A. Bonn, and W. N. Hardy, *Science* **300**, 1410 (2003).  
<sup>22</sup>T. T. Heikkilä, J. Särkkä, and F. K. Wilhelm, *Phys. Rev. B* **66**, 184513 (2002).  
<sup>23</sup>P. C. Howell, A. Rosch, and P. J. Hirschfeld, *Phys. Rev. Lett.* **92**, 037003 (2004).  
<sup>24</sup>R. Gross, L. Alff, A. Beck, O. M. Froehlich, D. Koelle, and A. Marx, *IEEE Trans. Appl. Supercond.* **7**, 2929 (1997); R. Gross and B. Mayer, *Physica C* **180**, 235 (1991).  
<sup>25</sup>B. H. Moockly, D. K. Lathrop, and R. A. Buhrman, *Phys. Rev. B* **47**, 400 (1993).